Selective Activation of ON and OFF Retinal Ganglion Cells to High-frequency Electrical Stimulation: A Computational Modeling Study

Tianruo Guo, *Student Member, IEEE,* Nigel H. Lovell, *Fellow, IEEE,* David Tsai, *Member, IEEE,* Perry Twyford, Shelley Fried, *Member, IEEE*, John W. Morley, Gregg J. Suaning, *Senior Member, IEEE* and Socrates Dokos, *Member, IEEE*

***Abstract*—In this study, ON and OFF retinal ganglion cell (RGC) models based on accurate biophysics and realistic representations of cell morphologies were used to understand how these cells selectively respond to high-frequency electrical stimulation (HFS). With optimized model parameters and the incorporation of detailed cell morphologies, these two models were able to closely replicate experimental ON and OFF RGC responses to epiretinal electrical stimulation. This modeling approach can be used to design electrical stimulus profiles capable of cell-specific activation, and is broadly applicable for the development of sophisticated stimulation strategies for visual prostheses.**

I. Introduction

Existing retinal visual prosthetic devices have limited ability to selectively or differentially electrically stimulate retinal neurons in clinical settings due to the relatively large area of retinal tissue activated by the electrodes. High-frequency stimulation (HFS) has been explored in cochlear prosthetics [1, 2]. It has also been used to induce selective conduction block in peripheral axon fibers [3]. A recent *in vitro* study suggested the possibility of employing 2 kHz HFS to maximize the difference in responses between ON and OFF retinal ganglion cell (RGC) types [4], underlying the possibility of HFS selectively activating different retinal neuron types.

Improved understanding on the underlying activation processes in RGCs is critical for further improvements in selectivity. Computational modeling approaches allow us to precisely control each biophysical and physical property, and isolate their effects in shaping RGC responses. If physiological response patterns in the retina can be more closely replicated and explained by a model, we can then optimize visual prosthesis stimulation parameters in order to improve therapeutic benefits.

In this study, we developed morphologically-detailed and biophysically-accurate ON and OFF RGC models to gain insights into the mechanisms underlying selective responses. Both models include accurate 3D morphological reconstruction, and their response behavior was optimized against multiple whole-cell recording datasets for accurate biophysics.

This research was supported by the Australian Research Council (ARC) through a Special Research Initiative in Bionic Vision Science and Technology grant to Bionic Vision Australia (BVA) and by NIH grants (EY023651 & EY019967) as well as by the US Veterans Administration (1I01RX000350)

T. Guo, D. Tsai, G. J. Suaning, N. H. Lovell and S. Dokos are with the Graduate School of Biomedical Engineering, University of New South Wales, Sydney, Australia. D. Tsai is also with the Howard Hughes Medical Institute, Biological Sciences and Bioelectronic Systems Lab, Electrical Engineering, Columbia University, New York, USA. J. W. Morley is with School of Medicine, University of Western Sydney, Australia. S. Fried and P. Twyford are with VA Boston Healthcare Systems, and the Department of Neurosurgery, Massachusetts General Hospital and Harvard Medical School, Boston, MA, USA

E-mail for correspondence: t.guo@unsw.edu.au

II. Methodology

A. Morphologically-realistic RGC models

The RGC ionic formulation used was an extension of the Fohlmeister and Miller (FM) description [5, 6]. Briefly, the ionic model included seven time-dependent membrane currents and one leakage current. We added a hyperpolarization-activated current (I_h) and a low-threshold voltage-activated calcium current (I_{CaT}) to the FM formulation. These two subthreshold currents have significant effects on RGC excitability [7, 8] and are thus likely to play important roles during electrical stimulation. Ionic channel conductances were set to be compartment-specific along the cell to reflect the proportion of ion channels in soma, dendrites, axon, hillock and axonal initial segment (AIS) regions of RGCs.

To develop accurate formulation of RGC geometries, rabbit ON and OFF cell morphologies were identified from their electrophysiology, dendritic field size/structure and stratification in the inner plexiform layer (IPL). Details of RGC model settings and cell morphological reconstructions can be found in [9]. Simulations were performed in NEURON 7.2 [10].

B. Extracellular Stimulation

The stimulation electrode in the model was defined by a circular disk electrode. The tissue was considered to be homogeneous. Under these conditions, the extracellular potential V at each point is defined by

$$V(r,z) = \frac{2I_o R_s}{\pi} \arcsin\left(\frac{2R}{\sqrt{(r-R)^2+z^2}+\sqrt{(r+R)^2+z^2}}\right) \qquad (1)$$

where r and z are the radial and axial distance respectively from the center of the disk for $z \neq 0$, R is the radius of the disk (R=15 μm), I_o is the stimulation current, R_s is the electrode

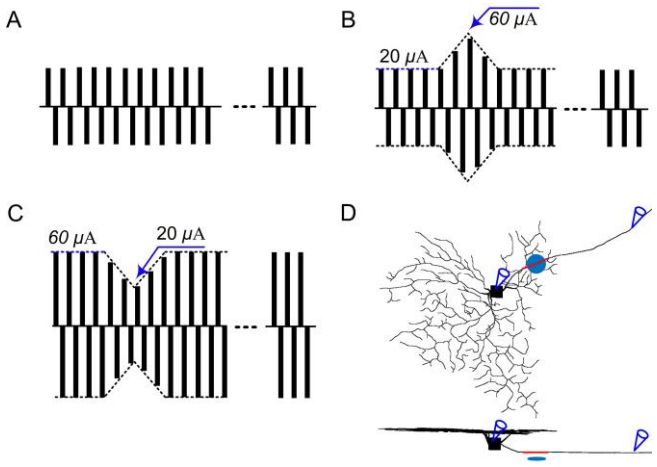

Figure. 1 Applied 2 kHz extracellular stimulus waveforms consisting of biphasic constant-current pulses of 100 μs per phase, with 160 μs cathodal-anodal inter-phase interval and 140 μs anodal-cathodal inter-phase interval. A. Constant-amplitude stimulation. B. Positive baseline amplitude modulation. Stimulation waveforms were reconstructed from the constant-amplitude stimulation in (A) with a 250 ms wide amplitude modulation 'diamond' with symmetric rise and fall phases. Baseline amplitude was 20 μA and the peak amplitude of the diamond was 60 μA. C. Negative baseline amplitude modulation with 60 μA baseline and 20 μA minimum amplitude as the diamond 'notch'. D. Simulated stimulus and measuring locations in the model OFF RGC. The epiretinal stimulation electrode (shown as a flat disk) was applied with 5 μm distance from center of the AIS (red compartment) and spiking responses were recorded in the soma and axon, shown by the cone-shaped electrodes.

transfer resistance (R_s=0.05 Ω). The stimulation electrode was centered epiretinally 5 μm above the center of the AIS. Electrical stimulation waveforms and parameters in this study were all adapted from the experimental study of Twyford *et al.*[4].

III. Results

A. Constant- amplitude stimulation

We simulated the response to 2kHz Lilly-type [11] biphasic stimulation (shown in Fig. 1A) in ON and OFF cells. The amplitude of the stimulus train remained constant within a given trial, but varied across trials ranged from 0 to 90 μA. Fig. 2 (A4) shows distinct non-monotonic spike-stimulus profiles for the ON and OFF RGC models. At low stimulus magnitudes, the spiking number typically increased with stimulus amplitude. However, as the amplitude increased further, the number of elicited spikes decreased substantially, creating a non-monotonic response profile. This is consistent with the recent *in vitro* studies [4]. We counted the total number of axonal spikes elicited over the 250 ms pulse train at each amplitude and plotted the total as a function of stimulus amplitude for both ON and OFF cells (Fig. 2 A4). The stimulus-response profiles demonstrated a distinct onset, width and amplitude, indicating their differential response to electrical stimulation between cells. The simulated soma and axon showed similar response patterns (see Fig. 2 A2).

B. Amplitude-modulated stimulation

To further validate the model, we measured the ON and OFF model axonal responses to two types of non-zero baseline amplitude modulation (shown in Fig. 1B and C). Fig. 2 (B2) illustrated the distinct ON and OFF cell responses. Stimulus baseline was fixed at 20 μA and the peak level was 60 μA (Fig. 1B). The ON cell response demonstrated an increased spiking rate during the diamond shaped modulation, returning to rest level as soon as the modulation was complete, while the OFF cell showed an opposite response pattern to that of the ON cell.

In another simulation, we reversed the amplitude levels of the baseline and the modulation peak. The baseline was fixed at 60 μA while the minimum 'notch' level was 20 μA (Fig. 1C). The inverted stimulus elicited the opposite response: there was a decrease in ON cell activity and an increase in OFF cell response during the diamond-shaped modulation (see Fig.2 B2, lower panels). All of these simulation results closely match the biological RGC responses (Fig. 2 B1) recorded under the similar stimulation conditions in [4], in which 40 μA baseline with a peak of 60 μA and 60 μA baseline with the minimum 'notch' of 40 μA were used.

C. Influence of active dendrites on non-monotonic profile

To investigate possible mechanisms underlying the non-monotonic response properties, we gradually removed the active dendritic tree by disconnecting dendritic branches from the full computer-reconstructed RGC geometry (Fig. 3B), and then examined somatic spiking in response to a range of HFS stimulation amplitudes. The simulation results indicated that the soma became more excitable with fewer dendrites, such that the non-monotonic (red) response profile changed into monotonic (black) with largely reduced dendritic branching, suggesting that dendritic structure may be a significant contributor of the non-monotonic nature of the HFS-based RGC responses.

IV. Discussion and Conclusion

To our knowledge, very little has been published on modeling of selective activation of functionally-distinct RGCs. This may be because existing RGC models do not consider the functional significance of cellular morphology and membrane channel distributions or kinetics in each cellular region. In this study however, with the optimized ionic channel distribution in each functional cellular area and incorporating detailed cell morphologies, we were able to reproduce the patterns of preferential excitation observed experimentally, as we adjusted the extracellular stimulus amplitude across a wide range of values.

We also used computational models to shed light on the likely mechanisms underlying the non-monotonic response profile, namely: why the RGCs demonstrated 'up and down' spiking response patterns as a function of stimulus amplitude, and how this property is affected by cell morphology and active cell properties.

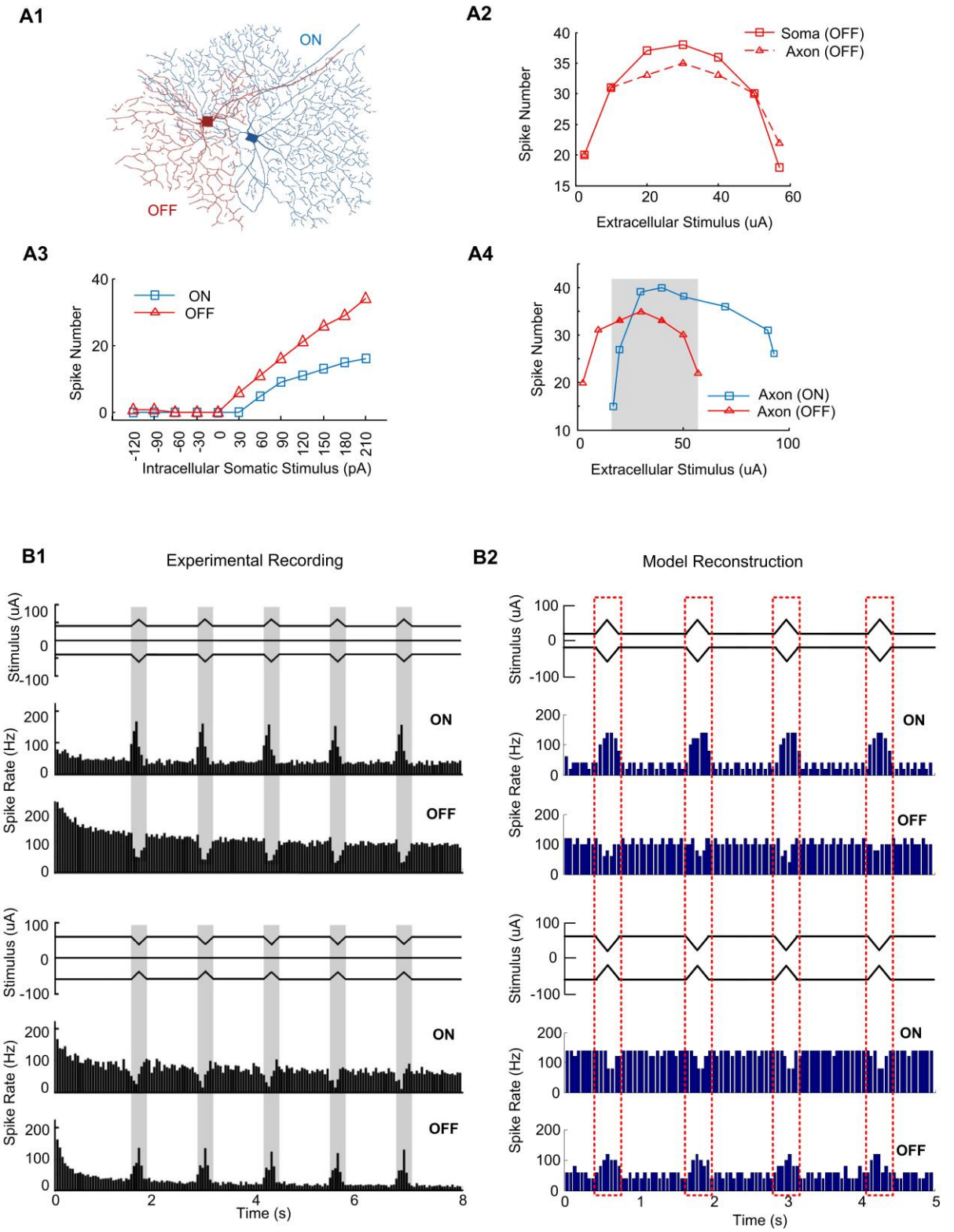

Figure. 2 Selective activation of ON and OFF RGCs to 2kHz HFS. A1. Model ON and OFF RGC morphologies. A2. Somatic and axonal response simulated in OFF RGC. A3. Difference in excitability between model ON and OFF RGC in response to intracellular somatic current injection. A4. Evoked axonal spiking numbers in model ON and OFF RGCs with constant-amplitude 2 kHz HFS (250 ms duration, 0~90 μA). Note that the shadow region can be used to adjust the extracellular stimulus range to selectively activate ON and OFF RGCs. B1. *In vitro* preferential ON and OFF RGC recruitment under HFS from [4]. Average spiking rates for ON (N=7) and OFF (N=7) cells in response to stimulus waveform shown at top (Upper panel: 40 μA baseline with a peak of 60 μA. Lower panel: 60 μA baseline with the minimum 'notch' of 40 μA). B2. Simulation results using realistic ON and OFF RGC models.

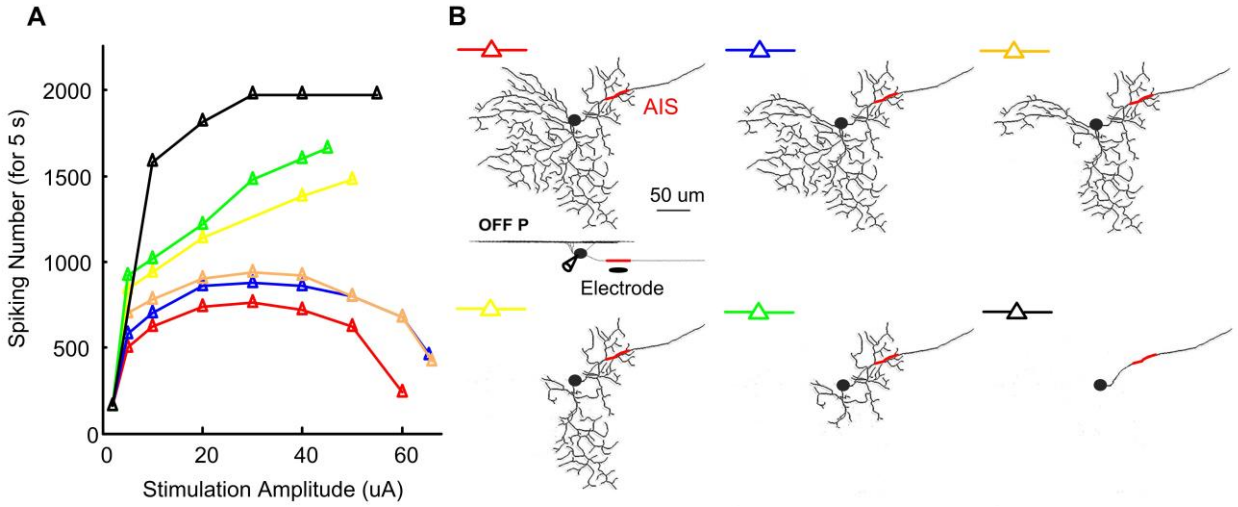

Figure. 3 Non-monotonic RGC spiking response pattern is altered by progressively removing active dendrites. A. Computationally simulated spiking numbers across 5 s trains of 2 kHz stimuli as a function of stimulus amplitude before (red) and after the removal of corresponding dendrites. The spiking number patterns (i.e. width and amplitude) were altered when dendritic branches were gradually removed. B. Cellular morphologies. Colors correspond to the different spiking pattern curves in (A).

Under simulations of dendritic pruning (Fig. 3), this response profile could be altered by gradually removing the active RGC dendritic structure, indicating that non-monotonic response properties are likely to result from active somato-dendritic interactions. Large dendritic loading can inhibit somatic excitation, and changing distribution of active conductances can further modify the shape of the response profile. On the other hand, the preferential activation (Fig. 2 B2) between ON and OFF model RGCs in response to amplitude-modulated HFS pulse trains is based on differences in onset, peak value and width of their characteristic non-monotonic response profiles (Fig. 2 A4). These differences are most likely to due to their unique ionic channel expressions and cell-specific morphologies. Differences in ionic channel properties between RGC types raise the possibility that each type may exhibit markedly selective firing patterns in response to the identical stimulation inputs. Neuronal morphologies can influence the flow of intracellular currents between neighboring compartments through their specific cell membrane area and intracellular resistivity. Further computational testing and experimental work will be required to isolate the effect of various cellular properties to better understand their contribution to the cell-spiking profiles observed.

Armed with these computational models, we can form a tight-loop investigation cycle, consisting of computational predictions on potentially beneficial stimulation strategies and experimental validations. These data-driven models can then provide a promising approach to rapidly probe the responses of identified RGCs to a broad range of novel stimulus configurations, as well as build constrained theories of selective RGC encoding.

In future studies, we also intend to expand our analysis and simulations to additional RGC types, in order to build comprehensive models of the electrical responses of the entire RGC population and further contribute to our understanding of retinal encoding and visual information processing.

REFERENCES

[1] L. Litvak, B. Delgutte, and D. Eddington, "Auditory nerve fiber responses to electric stimulation: modulated and unmodulated pulse trains," *J Acoust Soc Am,* vol. 110, pp. 368-79, 2001.

[2] L. M. Litvak, Z. M. Smith, B. Delgutte, and D. K. Eddington, "Desynchronization of electrically evoked auditory-nerve activity by high-frequency pulse trains of long duration," *J Acoust Soc Am,* vol. 114, pp. 2066-78, 2003.

[3] L. Joseph and R. J. Butera, "High-frequency stimulation selectively blocks different types of fibers in frog sciatic nerve," *IEEE Trans Neural Syst Rehabil Eng,* vol. 19, pp. 550-7, 2011.

[4] P. Twyford, C. Cai, and S. Fried, "Differential responses to high-frequency electrical stimulation in ON and OFF retinal ganglion cells," *J Neural Eng,* vol. 11, p. 025001, 2014.

[5] J. F. Fohlmeister and R. F. Miller, "Mechanisms by which cell geometry controls repetitive impulse firing in retinal ganglion cells," *J Neurophysiol,* vol. 78, pp. 1948-1964, 1997.

[6] J. F. Fohlmeister and R. F. Miller, "Impulse encoding mechanisms of ganglion cells in the tiger salamander retina," *J Neurophysiol,* vol. 78, pp. 1935-1947, 1997.

[7] S. C. Lee and A. T. Ishida, "Ih without Kir in adult rat retinal ganglion cells," *J Neurophysiol,* vol. 97, pp. 3790-3799, 2007.

[8] D. Henderson and R. F. Miller, "Low-voltage activated calcium currents in ganglion cells of the tiger salamander retina: experiment and simulation," *Vis Neurosci,* vol. 24, pp. 37-51, 2007.

[9] T. Guo, D. Tsai, J. W. Morley, G. J. Suaning, N. H. Lovell, and S. Dokos, "Cell-specific modeling of retinal ganglion cell electrical activity," *Conf Proc IEEE Eng Med Biol Soc,* vol. 2013, pp. 6539-42, 2013.

[10] M. L. Hines and N. T. Carnevale, "The NEURON simulation environment," *Neural Comput,* vol. 9, pp. 1179-209, 1997.

[11] J. C. Lilly, J. R. Hughes, E. C. Alvord, and T. W. Galkin, "Brief, Noninjurious Electric Waveform for Stimulation of the Brain," *Science,* vol. 121, pp. 468-469, 1955.